

## Timelike Compton Scattering with CLAS12 at Jefferson Lab

---

**Pierre Chatagnon\***

*IPN Orsay, for the CLAS collaboration*

*E-mail: [chatagnon@ipno.in2p3.fr](mailto:chatagnon@ipno.in2p3.fr)*

Generalized Parton Distributions (GPDs) [1, 2, 3, 4] describe the correlations between the longitudinal momentum and the transverse position of the partons inside the nucleon. At leading order, four quark helicity conserving GPDs ( $H$ ,  $\tilde{H}$ ,  $E$  and  $\tilde{E}$ ) per quark flavor describe the nucleon structure. For their direct relation to the angular momentum contribution of partons to the spin of the nucleon [5] and to the pressure distribution in the nucleon, GPDs have been at the center of many experimental programs. GPDs have been studied mainly using Deeply Virtual Compton Scattering (DVCS,  $ep \rightarrow e'p'\gamma$ ). Here we highlight the measurement of the time-reversal conjugate process of DVCS, Timelike Compton Scattering (TCS), using data taken by CLAS12. The experimental measurement of the TCS angular asymmetry will provide new information on the real part of GPDs. This proceeding assesses the current status of the TCS analysis and presents preliminary results based on CLAS12 data.

*Light Cone 2019 - QCD on the light cone: from hadrons to heavy ions - LC2019*

*16-20 September 2019*

*Ecole Polytechnique, Palaiseau, France*

---

\*Speaker.

## 1. Timelike Compton Scattering

The golden process to access GPDs is DVCS ( $ep \rightarrow e'p'\gamma$ ). For large enough photon virtuality  $Q^2$  and small  $-t \ll Q^2$ , DVCS is interpreted as an electron interacting with a single quark, which then re-emits a photon (see diagram in Figure 1). The DVCS amplitude depends on complex quantities called Compton Form Factors (CFFs) defined for the GPD  $H$  as:

$$\mathcal{H} = \sum_q e_q^2 \left\{ \mathcal{P} \int_{-1}^1 dx H^q(x, \xi, t) \left[ \frac{1}{\xi - x} - \frac{1}{\xi + x} \right] + i\pi [H^q(\xi, \xi, t) - H^q(-\xi, \xi, t)] \right\} \quad (1.1)$$

and similarly for other GPDs, where  $x \pm \xi$  are momentum fractions carried by the struck quark defined in Figure 1. DVCS observables measurements provide good constraints to the imaginary part of CFFs [6]. On the contrary the real part, directly linked to the pressure distribution in the nucleon, is much less known.

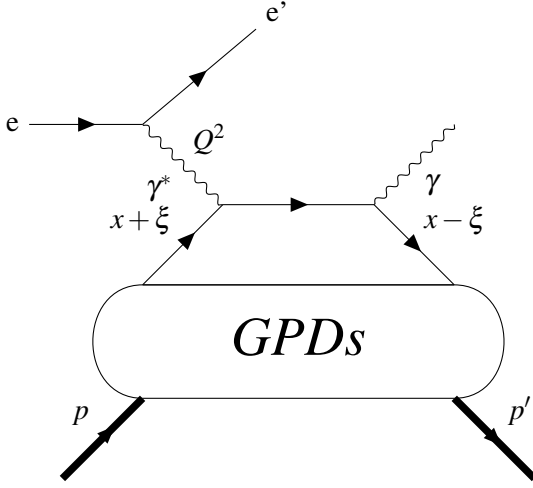


**Figure 1:** DVCS diagram at leading twist and leading order. At high photon virtuality  $Q^2$  and small transferred momentum  $-t = (p' - p)^2$  the interaction happens at quark level. The hit quark carries a momentum fraction  $x + \xi$  before the interaction,  $x - \xi$  after.

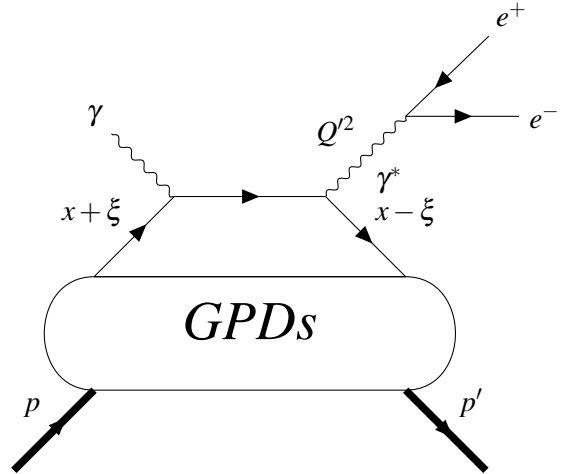


**Figure 2:** TCS diagram at leading twist and leading order. At high photon virtuality  $Q^2$  and small  $-t = (p' - p)^2$  the interaction happens at quark level.

As for DVCS, the Timelike Compton Scattering ( $\gamma p \rightarrow \gamma^* p' \rightarrow e^+ e^- p'$ ) amplitude depends on CFFs (see diagram in Figure 2). The cross-section of the photo-production of lepton pairs  $\gamma p \rightarrow e^+ e^- p'$  has contributions from TCS, from the Bethe-Heitler process and from their interference. Bethe-Heitler (BH) is the decay of the incoming real photon in a lepton pair, one of the leptons then interacting with the proton. The contribution of BH to the total cross section is at least ten times bigger than the TCS contribution [7, 8]. Thus direct measurement of the TCS contribution is difficult. However, the interference between BH and TCS gives direct access to the real part of the CFF  $\mathcal{H}$  via the ratio R proposed in [7]:

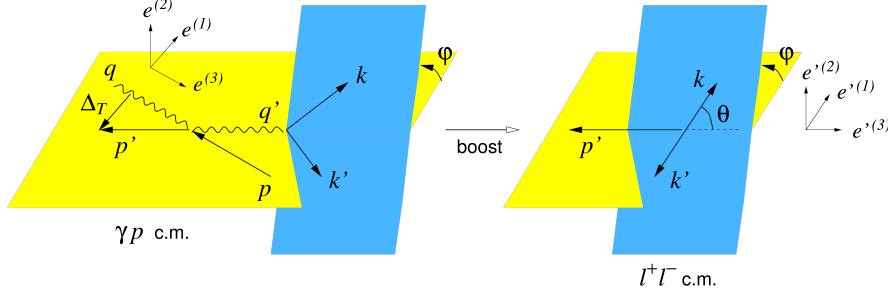


**Figure 3:** Definition of the kinematic variables for the  $\gamma p \rightarrow \gamma^* p' \rightarrow e^+ e^- p'$  reaction (Figure extracted from [7]). The hadronic plane in yellow is defined by the momenta of the incoming and outgoing proton in the  $\gamma p$  center-of-mass frame. The leptonic plane in blue is defined by the lepton-pair momenta.

$$R(\sqrt{s}, Q^2, t) = \frac{\int_0^{2\pi} d\phi \cos(\phi) \frac{dS}{dQ^2 dt d\phi}}{\int_0^{2\pi} d\phi \frac{dS}{dQ^2 dt d\phi}} \quad (1.2)$$

where

$$\frac{dS}{dQ^2 dt d\phi} = \int_{\pi/4}^{3\pi/4} d\theta \frac{L}{L_0} \frac{d\sigma}{dQ^2 dt d\phi d\theta} \quad (1.3)$$

with  $L = \frac{Q^2 - t)^2 - b^2}{4}$ ,  $L_0 = \frac{Q^4 \sin^2 \theta}{4}$ ,  $b = 2(k - k')(p - p')$ , and  $k, k', p, p', \theta, \phi$  are defined in Figure 3. Exploratory TCS measurements have been performed with the CLAS detector [9].

## 2. Data analysis

### 2.1 The CLAS12 detector

The angular modulation of the TCS cross section will be measured from data taken by the CLAS12 detector at Jefferson Lab. It collected data on proton target in 2018, with a 10.6 GeV electron beam. CLAS12 comprises tracking and Time-of-Flight (TOF) for heavy particle identification. It uses Cherenkov detectors and electromagnetic calorimeters for lepton identification. Charge and momentum reconstruction is possible using a toroidal magnetic field. Two field polarities were used: negative charge particles inbending and outbending.

### 2.2 Events selection

Events with a lepton pair and a proton were selected from the complete data set. Protons are identified by matching the time-of-flight measured by the TOF detectors and the one calculated from the reconstructed momentum. The identification of leptons relies on tracking for charge and momentum determination. Cherenkov and Calorimeters are used to reject pions. TCS is accessible in the photo-production of a lepton pair off a proton, while in our experiment we have an electron beam impinging on a proton target. We thus select events where the beam electron radiated a real photon, that then interacts with a target proton. The electron is then scattered at a very low angle

and stays undetected. The four-momentum of the scattered electron that radiated the real photon can be determined as:

$$p_{scat. e^-}^\mu = p_{beam}^\mu + p_{target}^\mu - p_{proton}^\mu - p_{e^+}^\mu - p_{e^-}^\mu. \quad (2.1)$$

The missing mass of the scattered electron ( $M_{scat. e^-}^2 = p_{scat. e^-}^2$ ) is required to be close to zero. The transverse momentum fraction of the missing particle is cut around zero to ensure that a real photon is emitted.

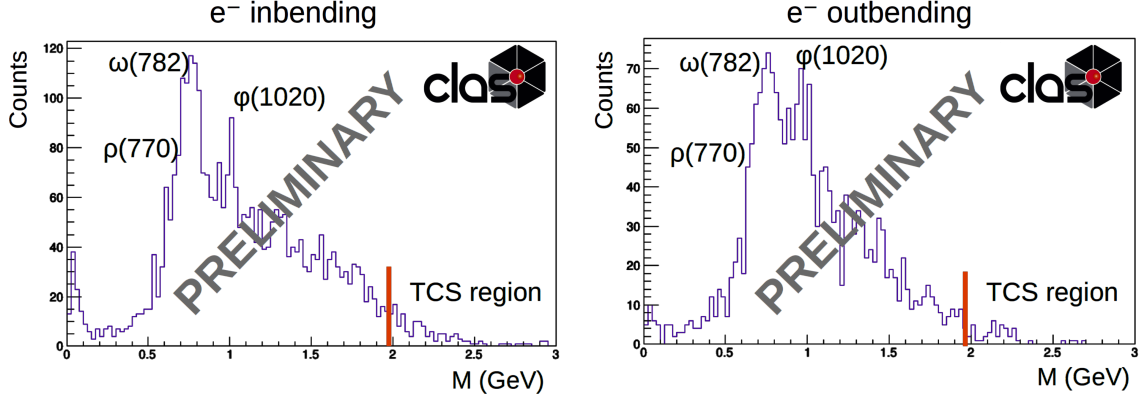


**Figure 4:** Lepton-pair invariant mass for the two torus magnetic field polarities. The events in the 2-3 GeV region are selected for the measurement.

The invariant mass of the lepton pair  $M_{pair}^2 = (p_{e^+}^\mu + p_{e^-}^\mu)^2$  after exclusivity cuts is shown in both torus magnetic field configurations in Figure 4. The low mass region is dominated by vector-meson resonances ( $\rho(770)$ ,  $\omega(782)$ , and  $\phi(1020)$ ). In the analysis, we select events in the 2-3 GeV region to avoid resonances. The data set shown here corresponds to approximately 6% of the total amount of collected data currently being processed.

### 3. Projected results

From the data shown in Figure 4, 4000 events are expected in the selected mass range out of the whole data set. The achievable statistical precision with the current available data set is estimated by simulating  $\gamma p \rightarrow e^+ e^- p'$  reaction weighted by BH and TCS/BH interference term. The GPDs double distribution parametrization [10] is used to calculate the interference weight. The strength of the D-term can be varied with a multiplying factor  $\kappa$  as:

$$H(x, \xi, t) = H_{DD}(x, \xi, t) + \kappa \frac{1}{N_f} \Theta(\xi - |x|) D\left(\frac{x}{\xi}, t\right) \quad (3.1)$$

where  $H_{DD}(x, \xi, t)$  is the double distribution parametrization of the GPD,  $N_f$  is the number of active flavors and  $\kappa$  is the D-term strength (see [7]). The R ratio (equation 1.2) is obtained in the CLAS12 acceptance as a function of  $-t$  for three different values of  $\kappa$  and for BH-only weighted events. Results are displayed in Figure 5, including projected error bars. Our measurement is expected to provide a good insight on the strength of the D-term.

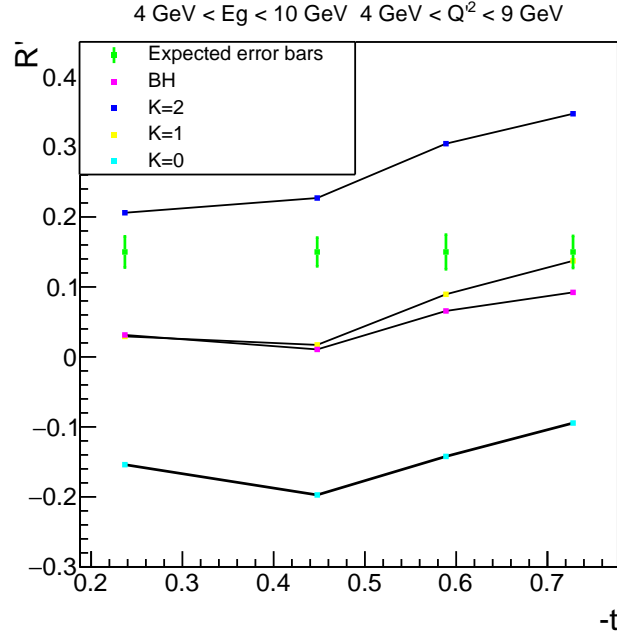


**Figure 5:** The ratio  $R$  calculated as a function of transferred momentum  $t$  in the CLAS12 acceptance for different strengths of the D-term and for BH-only weighted events. The values of  $R$  for the green dots are arbitrary, and the error bars correspond to the expected statistical errors achievable for the current data set taken by CLAS12.

## References

- [1] A. V. Radyushkin. Nonforward parton distributions. *Phys. Rev.*, 56:5524–5557, Nov 1997.
- [2] Michel Guidal, Hervé Moutarde, and Marc Vanderhaeghen. Generalized parton distributions in the valence region from deeply virtual compton scattering. *Reports on Progress in Physics*, 76(6):066202, 2013.
- [3] M. Diehl. Generalized parton distributions. *Physics Reports*, 388(2):41 – 277, 2003.
- [4] Markus Diehl. Introduction to gpdfs and tmfdfs. *The European Physical Journal*, 52(6):149, Jun 2016.
- [5] Xiangdong Ji. Gauge-invariant decomposition of nucleon spin. *Phys. Rev. Lett.*, 78:610–613, Jan 1997.
- [6] Nicole d’Hose, Silvia Niccolai, and Armine Rostomyan. Experimental overview of deeply virtual compton scattering. *The European Physical Journal*, 52(6):151, Jun 2016.
- [7] E.R. Berger, M. Diehl, and B. Pire. Timelike compton scattering: exclusive photoproduction of lepton pairs. *The European Physical Journal*, 2, 2002.
- [8] Boer, M., Guidal, M., and Vanderhaeghen, M. Timelike compton scattering off the proton and generalized parton distributions. *Eur. Phys. J.*, 51(8):103, 2015.
- [9] R. Parnuzyan. *Timelike Compton Scattering*. PhD thesis, Yerevan Physics Institute, 2010.
- [10] A. V. Radyushkin. Double distributions and evolution equations. *Phys. Rev.*, 59:014030, Dec 1998.